

On the power spectrum of motor unit action potential trains synchronized with mechanical vibration

Maria Romano, Antonio Fratini, *Member, IEEE*, Gaetano D. Gargiulo, *Member, IEEE*, Mario Cesarelli, Luigi Iuppariello, and Paolo Bifulco*

Abstract - Objective: Provide a definitive analysis of the spectrum of a motor unit action potential train elicited by mechanical vibratory stimulation via a detailed and concise mathematical formulation. Experimental studies demonstrated that motor unit action potentials are not exactly synchronized with the vibratory stimulus but show a variable latency jitter, whose effects have not been investigated yet. **Methods:** Synchronized action potential train was represented as a quasi-periodic sequence of a given motor unit waveform. The latency jitter of action potentials was modeled as a Gaussian stochastic process, in accordance to previous experimental studies. **Results:** A mathematical expression for power spectrum of a synchronized motor unit action potential train has been derived. The spectrum comprises a significant continuous component and discrete components at the vibratory frequency and its harmonics. Their relevance is correlated to the level of synchronization: the weaker the synchronization, the more relevant the continuous spectrum. EMG rectification enhances the discrete components. **Conclusion:** The derived equations have general validity and well describe the power spectrum of actual EMG recordings during vibratory stimulation. Results are obtained by appropriately setting the level of synchronization and vibration frequency.

Significance: This study definitively clarifies the nature of changes in spectrum of raw EMG recordings from muscles undergoing vibratory stimulation. Results confirm the need of motion artifact filtering for raw EMG recordings during stimulation and strongly suggests to avoid EMG rectification that significantly alters the spectrum characteristics.

Index Terms—EMG spectrum, motion artifact, motor unit action potential train, whole body vibration

I. INTRODUCTION

MECHANICAL vibrations applied to skeletal muscles elicit a reflex contraction known as the tonic vibration reflex (TVR). TVR mainly arises from the activity of the intrafusal muscle spindle's Ia fibers (naturally sensitive to muscle stretch), which can be modulated by external applied vibration [1, 2]. The discharge rate of muscle spindles is indeed modified as result of vibratory stimulation when marked muscle length changes are recorded [3-5]. Interestingly, spindles reveal a one-

to-one response to each cycle of a sinusoidal vibration up to about 100 Hz [6].

Muscle spindle's Ia fibers are excitatory afferents for the corresponding alpha motor neuron, however they are only one of the motor neuron's afferent inputs and can only facilitate its firing. Supraspinal signals, Ib afferents and other sensory pathways (either monosynaptic or polysynaptic) also provide other sources of input [7].

The Motor Unit (MU) activity may be modulated by the mechanical vibration; proof of synchronization can be found in the existing literature where single MUs' action potentials (MUAP) have been directly recorded with thin wire electrodes placed into muscles [8-14].

TVR and the relative MU synchronization, are often cited as working principle for Whole Body Vibration (WBV) treatments. In WBV, mechanical vibration is delivered to the whole patient's body (as opposed to local stimulation) via oscillating platforms on which the subject can stand, or hold various postures. Although a proper TVR requires the stimulus to be applied at the tendons or muscle level and target a single muscle or group [15], this convenient vibration delivery method has made WBV a popular complement, or even an alternative, to physical training and rehabilitation [16, 17].

To assess and measure muscular response during stimulation, surface EMG and its RMS are largely utilized as evidence of WBV efficacy [18]. Ambiguities and contradictions however arise in assessing EMG recordings during vibration treatments since the periodic component of the EMG power spectrum is linked with a strong motion artifact induced by the vibration itself [3, 13, 19-23]. Artifacts are generated by the relative motion between electrodes and the underlying tissues, the mechanical alterations induced between skin layers, and the stretching of the skin under the electrodes. Motion artifacts appear as cyclic waveforms at the vibration frequency superimposed to the EMG signal and the resultant spectrum shows sharp impulses at the vibration frequency and its harmonics.

Not all the existing literature however contemplates the motion artifacts contribution, and most of the spectrum changes

*P. Bifulco (correspondence e-mail: paolo.bifulco@unina.it), L. Iuppariello and M. Cesarelli are with the Dept. of Electrical Engineering and Information Technologies, University Federico II, Naples, Italy, A. Fratini is with the School of Life and Health Sciences, Aston University, Birmingham, United

Kingdom. G. D. Gargiulo is with Wester Sydney University, Penrith, Australia and M. Romano is with the Dept. of Experimental and Clinical Medicine, University Magna Graecia, Catanzaro, Italy.

are attributed to MUAP synchronization [24, 25]. Indeed, MUs exactly synchronized with the vibration stimulus generate rigorously periodical MUAP trains (MUAPT) and their spectrum is discrete (i.e. concentrated at the harmonics of the vibration frequency). This conclusion is debatable, and concerns were also raised on experimental recording methodology [26].

Moreover, alpha motor neurons cannot respond to frequencies higher than 50 Hz [27]. They can eventually synchronize at sub-harmonic frequencies if vibratory stimulation exceeds those values. Even in this case however, MUAPT should result periodic and the relative spectrum discrete. Actually, the actual spectrum of EMG recordings under vibratory stimulation consist of both discrete and continuous components.

Taking into account the physiology of muscle contraction summarized above and the presence of artifacts, it is reasonable to consider both components as parts of the surface EMG signal [28]. Discerning between the two contributions is however challenging: artifacts and MUAPs are both synchronized with the vibration frequency, therefore their spectra overlap and artifact filtering strategies using notch or comb filters inevitably remove part of the genuine EMG signal [3, 20-22, 28].

This study aimed at obtaining a definitive analysis of the MUAPT spectrum during vibratory stimulation via a detailed mathematical formulation considering the peculiar variable synchronization revealed by direct experimental MU recordings found in literature. Concise formulation of MUAPT signal and strict mathematical computations are provided in the Methods and Appendix sections. Conclusive mathematical formulation and derived analyses on spectrum contents variations (continuous vs discrete) are presented in the Results section.

In summary, this study revealed that the actual, non-exact synchronization of a MUAP with the vibration cycles (i.e. the latency jitter) contributes to broaden the spectrum, no longer concentrated at the vibration frequency and its harmonics only.

It is worth clarifying that this study focused on MUAP trains synchronized with vibration and does not intend to analyze the effect of other non-synchronous MUs that can coexist within EMG.

II. METHODS

In this section, the elements for a concise mathematical formulation of MUAPT under vibratory stimulation are proposed. MUAP was formalized as derivative of Gaussian pulses and synchronization jitter was modeled as a stochastic process. A concise form for MUAPT expression was finally derived to assess the effects on MUAPT, and in turn on EMG spectrum.

A. Motor unit action potential

The MUAP waveform, i.e. the voltage recorded by the depolarization of the specific MU at the recording site, depends on the relative positioning between the electrodes and the MU muscle fibers, and can have different shapes (i.e. biphasic, triphasic or polyphasic).

In this study biphasic MUAP waveforms were mainly considered, in accordance to real recordings [29], however results are easily generalizable to other waveforms.

A biphasic MUAP waveform can be obtained as the derivative of a Gaussian pulse:

$$m(t) = \frac{d}{dt} p(t) = \frac{d}{dt} \left(\frac{1}{\lambda\sqrt{2\pi}} e^{-\frac{t^2}{2\lambda^2}} \right) = -\frac{t}{\lambda^3 \cdot \sqrt{2\pi}} \cdot e^{-\frac{t^2}{2\lambda^2}} \quad (1)$$

$$\leftrightarrow M(\omega) = -\frac{\omega}{\lambda^2} \cdot e^{-\frac{\omega^2 \lambda^2}{2}}$$

Whereas $m(t)$ represents the MUAP waveform in time domain (obtained differentiating a Gaussian pulse $p(t)$) and $M(\omega)$ its spectrum ($\omega=2\pi f$), λ determines the time duration of the MUAP. Equation 1 provides a simple, yet realistic representation of a MUAP and its Fourier transform, the reader can find more accurate simulations and sophisticated MUAP descriptions in literature [30, 31]. Fig. 1 shows an example of biphasic MUAP (panel a, solid line) and its spectrum (panel b, solid line) obtained using equation 1: in this example λ is set to 1.5 ms that correspond to a MUAP duration of about 12 ms (in accordance to [32-38]). As it is possible to infer from the figure, the MUAP Fourier transform resembles the typical EMG spectrum.

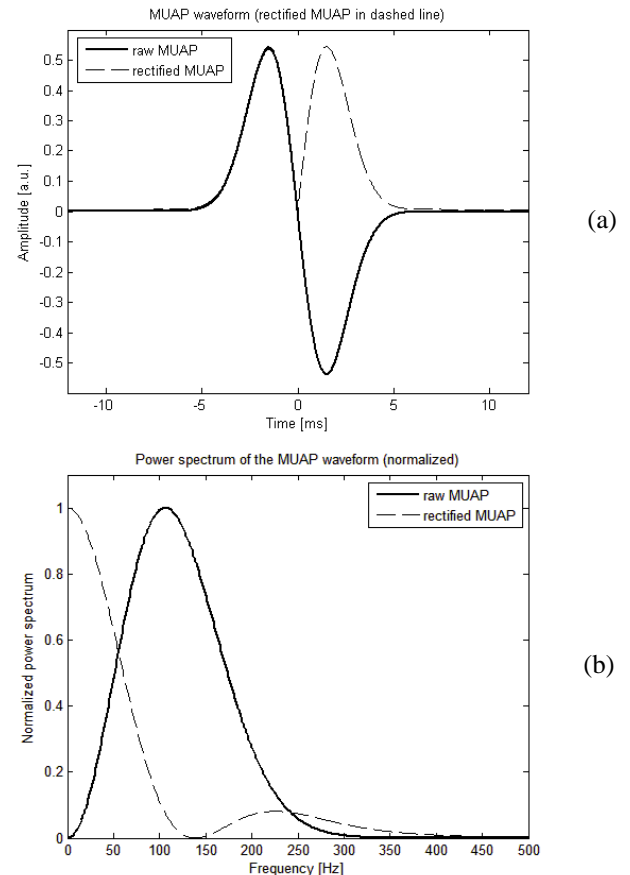


Fig. 1. (a) Biphasic MUAP waveform; (b) Normalized power spectrum of the MUAP. Rectified version of the MUAP and its power spectrum are shown superimposed to the previous images as dashed lines.

Moreover, since some authors use the rectified EMG signal

instead of the raw EMG [29], the rectified version of the MUAP waveform and its spectrum were also computed and reported in Fig. 1 (dashed lines) to facilitate comparison.

Rectification is a non-linear operator and alters the EMG power spectrum [29, 30]. The rectified EMG spectrum content is concentrated more towards low frequencies (see Fig. 1b).

B. MUAP latency modeling

The variability of MUs activation time with respect to the stretch stimulus strongly affects the spectrum of EMG signal related to the synchronized MUs. A proper mathematical formulation of MUAPT is indeed necessary. During vibratory stimulation, the discharge patterns of motor neurons correlate with the vibratory pulses, however MUAPs show a variable latency jitter with respect to the vibration cycle onset [8]. Actually, there is not a unique or precise phase relationship between MUAP and the vibration period but rather a statistically significant link. Fig. 2 reports an example of temporal distribution of MUAPs related to the vibration cycle.

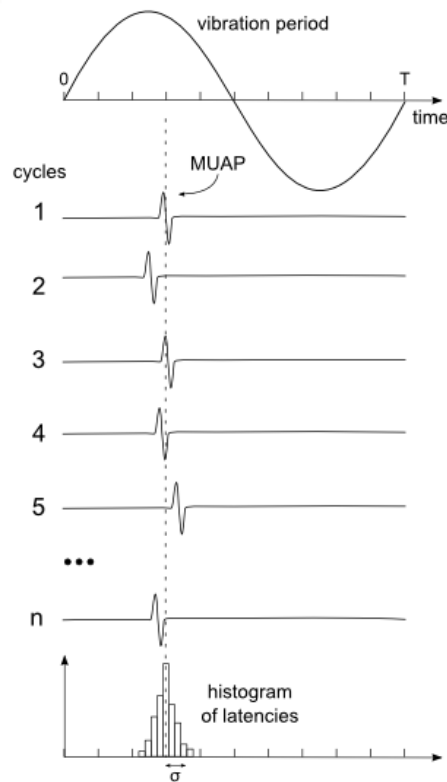


Fig. 2. Sketch of the activity of a single motor unit during muscle mechanical vibration. The figure is based on real data recorded in vivo with wire electrodes (e.g. [8]). The top trace depicts the vibration cycle, the following resemble the recording of MUAP relative to n vibration cycles. A part a given, constant delay from the vibration onset, the MUAPs do not show a perfect phase-lock to the vibration but rather a variable latency jitter. At the bottom a histogram of the latencies, as those provided by different studies [8, 13, 19, 39] based on a large number of recordings is depicted.

Standard Deviation (SD) of the latencies of the MUAP has been investigated for different muscles as a function of the vibration frequency and has been found dependent on the stimulus frequency. At low vibration frequencies, the stimulus period is indeed long enough for both monosynaptic and polysynaptic events to occur, spreading the latency jitter [9, 12,

14]. In more details, SDs of latency have been found ranged 0.4 - 1.3 ms at 83 Hz [8], while lower vibration frequencies correlate with increased SDs; 3 ms were reported at 30 Hz [39]. A study that combined experimental recording and EMG simulation considered even wider SDs of latency reaching up to 6 ms [23].

In this study, latency jitter of the MUAP was modeled as a sequence of independent, identically distributed (IID) samples taken from a strictly stationary continuous stochastic (SSS) process α .

$$\alpha \approx N(0, \sigma^2) \leftrightarrow \alpha(t) = \frac{1}{\sigma \cdot \sqrt{2\pi}} \cdot e^{-\frac{t^2}{2\sigma^2}} \quad (2)$$

The process α accounts for the not exact synchronization and can be assumed normally distributed with a zero mean and variance σ^2 (Fig. 2):

C. Actually synchronized MUAP train description

According to experimental recordings, a single MUAPT (reported here as $x(t)$) synchronized with a vibration can be assumed as a time series of given MUAP waveforms $m(t)$ and written as:

$$x(t) = \sum_k m(t - kT_s - \alpha_k) \quad (3)$$

Where T_s is the period of the stimulus; k is an integer number that represents the iteration and α_k is the specific latency jitter of the alpha motor neuron k^{th} action potential.

MUAPT signal can be equivalently obtained as a convolution product between a Dirac impulses train $r(t)$ and the MUAP waveform $m(t)$ or, equally, as the output of a linear time-invariant filter with a sequence of Dirac delta functions as input [40-42]:

$$x(t) = r(t) * m(t) \quad (4)$$

Whereas $r(t)$ is the impulses train and the asterisk represents the convolution product:

$$r(t) = \sum_k \delta(t - kT_s - \alpha_k) \quad (5)$$

Using equation 4 the spectrum of the MUAPT $x(t)$ can be obtained by multiplying the Fourier transforms of the impulses sequence $r(t)$ and the MUAP waveform $m(t)$.

III. RESULTS

Beginning from the equations 3 and 4, and after some mathematical manipulations, $S_{xx}(f)$ the power spectrum of the actually synchronized MUAPT signal $x(t)$ has been formalized. The details of the entire procedure are reported in the appendix.

$S_{xx}(f)$ is given by:

$$S_{xx}(f) = \frac{|M(f)|^2}{T_s} \cdot \left[1 - |A(f)|^2 + \frac{|A(f)|^2}{T_s} \cdot \sum_k \delta\left(f - \frac{k}{T_s}\right) \right] \quad (6)$$

The second term of equation 6 can, for simplicity of explanation, be divided in two factors:

$$factor_1 = \frac{|M(f)|^2}{T_s}$$

$$factor_2 = \left[1 - |A(f)|^2 + \frac{|A(f)|^2}{T_s} \cdot \sum_k \delta \left(f - \frac{k}{T_s} \right) \right]$$

Whereas $A(f)$ is the Fourier transform of the zero-mean Gaussian PDF of the α stochastic process representing the latency jitter of the MUAP (eq. 2). In particular, given that the Fourier transform of a Gaussian remains Gaussian, $A(f)$ is:

$$\alpha(t) = \frac{1}{\sigma \cdot \sqrt{2\pi}} \cdot e^{-\frac{t^2}{2\sigma^2}} \leftrightarrow A(f) = e^{-\frac{4\pi^2 f^2 \sigma^2}{2}} \quad (7)$$

Equation 6 clearly shows that the power spectrum of an actually synchronized MUAPT comprises both a continuous and a discrete component (factor 2) multiplied by the MUAP spectrum $M(f)$ (factor 1).

Focusing only on factor 2, it is easy to recognize that the continuous part is given by the first two addenda and depends on the σ of the Gaussian distribution: the larger is its standard deviation the wider is the spectrum.

In details, the weaker is the synchronization of the MUAPs with the mechanical vibration, the more relevant becomes the continuous part of the power spectrum. If the MUAPs are instead perfectly synchronized (i.e. the standard deviation of α is zero) the spectrum comprises only the discrete addendum. Note that the discrete part of the power spectrum is limited to the vibration frequency and its harmonics, as expected.

The power spectrum of the actually synchronized MUAPT is therefore the sum of impulses (discrete component) and a continuous component distributed across all frequencies. The continuous component becomes predominant at higher frequencies while the discrete is greater at low frequencies.

A graphical representation of the factor 2 of the equation 6 is reported in Fig. 3. In this example the SD of the latency jitter (the σ in equation 7) of a MUAP is set to 3 ms and the vibration frequency to 25 Hz.

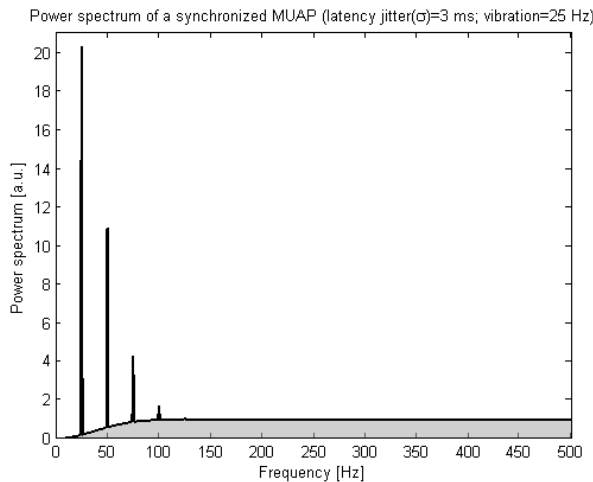


Fig. 3. Example of the power spectrum of a MUAP train (see equation 6, only factor 2, and equation 7) without considering the filtering effect due to MUAP waveform. The SD of the MUAP latency jitter was set to 3 ms and the vibration frequency was set to 25 Hz.

Percentage of the signal power contained at the vibration frequency and its harmonics with respect to the total power was

calculated. This is particularly important when these tiny bands are suppressed by notch, comb filters to reduce motion artifacts. Clearly, this percentage depends on the level of synchronization.

Fig. 4 shows the percentage of the continuous power spectrum with respect to the SD of the MUAP latency jitter. The complement to 100 of this percentage represents the power of the MUAPT at the vibration frequency and its harmonics. The figure includes a series of curves obtained by integrating the power spectrum within different bands of interest (i.e. 0-250, 0-300, 0-350, 0-400, 0-450 Hz).

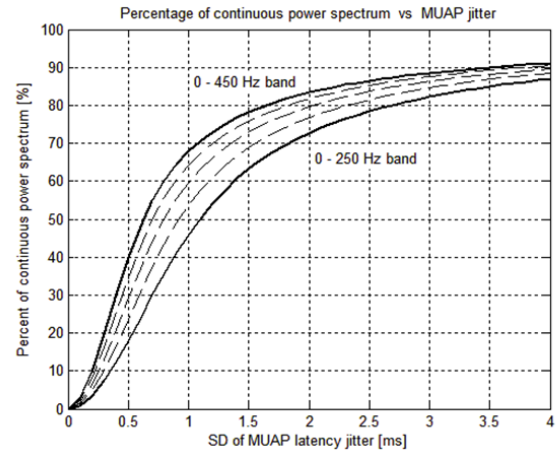


Fig. 4. Percentage of the continuous power spectrum (equation 6, only factor 2) with respect to the SD of the MUAP latency jitter. The successive five curves from the bottom upwards were obtained by integrating the power spectrum within different bands of interest: 0-250, 0-300, 0-350, 0-400, 0-450 Hz.

If the SD is equal to 0 there is a perfect synchronization of the MUAP with the vibration (exact phase-lock), the MUAPT is periodic and therefore all the power is concentrated at the vibration frequency and its harmonics (there is not a continuous spectrum). When the latency jitter increases, more a more power is spread into the continuous part of the spectrum. The continuous spectrum becomes already relevant (more than the 50%) for SD values greater than 1 millisecond.

With latency jitters values of about 3 ms (associated with the commonly utilized WBV frequencies) the continuous spectrum contains about 85% of the total power. Percentages tend asymptotically to 100% for greater SDs.

Finally, to obtain the MUAPT spectrum and assess the overall variations, we need to multiply both factors (i.e. multiply factor 2 by the spectrum of the MUAP waveform $M(f)$). Actually, factor 1 simply acts as a filter. Although individual MUAP waveform can vary, the spectrum is contained within that of the EMG. Without loss of generality, Fig. 5a shows the final spectrum obtained by multiplying the spectrum represented in Fig. 3 with that of the MUAP represented in Fig. 2(a), to provide an effective example. Similarly, Fig. 5b shows the final spectrum when the rectified MUAP waveform is considered.

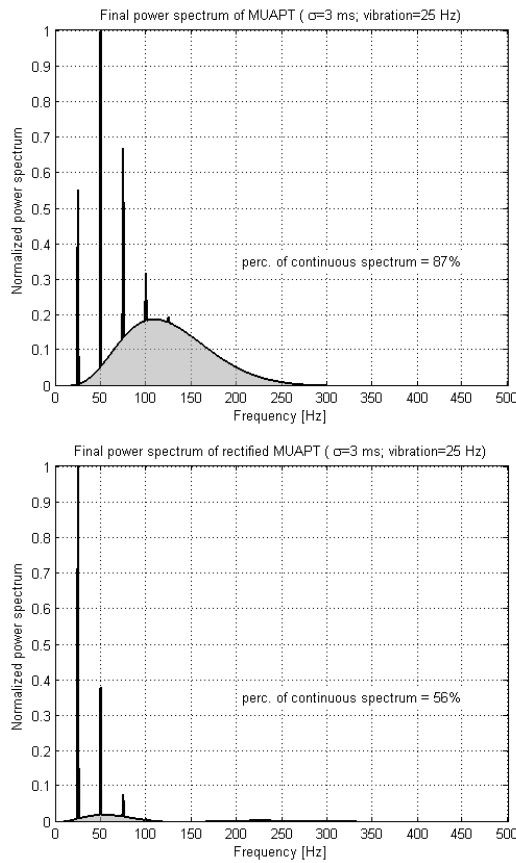


Fig. 5. Example of the final power spectrum of a MUAP train (a) and its rectified version (b). The MUAP waveform has been obtained by equation 5 with λ set to 1.5 ms. SD of the MUAP latency jitter was set to 3 ms, the vibration frequency to 25 Hz.

As before (see Fig. 4), the percentage of the power contained in the continuous spectrum taking into account the MUAP waveform can be re-calculated by varying the latency jitter. Results are shown in Fig. 6.

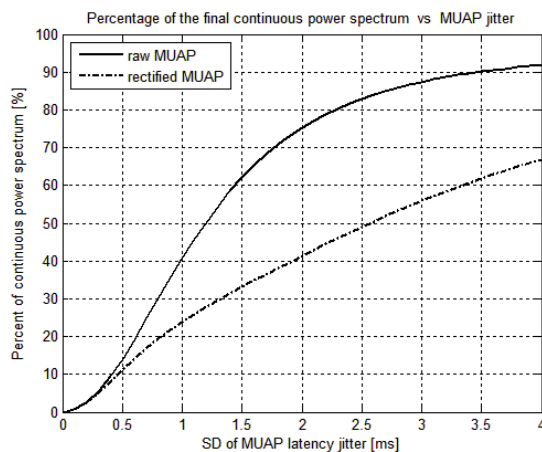


Fig. 6. Percentage of the continuous power spectrum with respect to the SD of the MUAP latency jitter. MUAP waveform influence is here reported: the solid line is obtained by using the raw MUAP, while the dashed and dotted line is obtained by using the rectified MUAP.

The solid-line curve was obtained using the raw MUAP as described in equation 5 with λ set to 1.5 ms. The dash-dotted

line was instead obtained using the rectified MUAP. With the rectified MUAP the final spectrum is different and increased at the lowest frequencies (see Fig. 2b), where the discrete peaks are dominant, whereas it is attenuated at central frequencies. As a consequence, by using rectified EMG the power of the continuous spectrum is smaller.

Table 1 concisely shows the percentage of continuous spectrum values obtained by varying the MUAP duration and its shape. Similarly, to the biphasic waveform (see eq. (1) and Fig.1), a triphasic MUAP waveform was modeled as the second derivative of the Gaussian pulse. The far right column values were obtained using a rectified version of the selected MUAP. All data are calculated for a SD of MUAP latency jitter of 3 ms.

TABLE I

MUAP type	value of λ [ms]	MUAP duration	Continuous spectrum at $\sigma = 3$ ms	Continuous spectrum (rectified)
bi-phasic	1.0	8 ms	93 %	66 %
bi-phasic	1.5 *	12 ms	87 %	56 %
bi-phasic	2.0	16 ms	78 %	49 %
bi-phasic	2.5	20 ms	71 %	44 %
bi-phasic	3.0	24 ms	62 %	42 %
tri-phasic	1.0	8 ms	96 %	68 %
tri-phasic	1.5	12 ms	94 %	58 %
tri-phasic	2.0	16 ms	91 %	51 %
tri-phasic	2.5	20 ms	86 %	47 %
tri-phasic	3.0	24 ms	79 %	46 %

Percentages of the continuous spectrum at $\sigma=3$ ms when changing MUAP duration ϵ and shape. (*) corresponds to the λ considered for the waveform in Fig. 1.

IV. DISCUSSION

This study provides a mathematical formulation of the power spectrum of action potential trains of a motor unit actually synchronized with mechanical vibration. Indeed, as reported by previous experimental studies involving direct measurement with needle electrodes under mechanical vibratory stimulation, the synchronization of the relative α motor neuron shows a variable latency.

The results of this study are of particular importance since clarify the nature of the variations in spectrum of raw EMG recordings of muscles undergoing vibratory stimulation. The derived equations have a general validity, but it is worth analyzing the effect of the latency jitter on practical cases.

There is in fact an ongoing debate on whether the increased power at the vibration frequency and harmonics is due to motor unit synchronization or rather to the motion artifact. Reasonably, both effects are present.

An exact synchronization (i.e. a pure periodic signal) of motor unit activity can only produce a discrete spectrum at the fundamental vibration frequency and its harmonics. Instead, the natural latency jitter of the synchronized MUs spreads the spectral power density over a larger band as sum of discrete components (impulses) and a continuous contribution distributed across all frequencies.

Using the concise formulation derived within this study, a quantitative analysis was performed and the power ratio of the continuous part of the spectrum (with respect to the whole

spectrum) computed by varying the degree of motor unit synchronization. This is either dependent on the standard deviation of the latency jitter and on the possible rectification applied to the raw recording.

In WBV treatments the vibration frequencies are confined below 45Hz with latency jitter of few milliseconds (e.g. 3 ms at 30 Hz). In this case, using our mathematical model, the spectrum is predominantly continuous with only a small amount pertaining to vibration frequency and its harmonics. This justifies the use of notch filters to eliminate the motion artifact embedded in the EMG recordings.

Moreover, rectification consistently alters the action potential spectrum, which appears concentrated towards lower frequencies, and reduces the continuous spectrum contribution. Indeed, the rectification introduces undesired filtering of the central frequencies of the EMG (resulting in an overall smaller percentage of the power in the continuous spectrum) and, at the same time, enhances the lower frequencies where the discrete spectrum and the motion artifact are relevant. The intensity of the motion artifact is usually unknown but certainly contributes to overestimate the muscle response to vibration.

For applications involving higher vibration frequencies, it is reasonable to consider the motor unit synchronized with sub-harmonics of the vibration frequency, as α motor neuron maximum firing rate is limited. In this case our model remains valid if a sub-harmonic is used for simulations instead of the vibration frequency itself. Moreover, at higher vibration frequencies (e.g. greater than 50 Hz [8]) latency jitters are smaller and a greater percentage of the power density belongs to the discrete spectrum. In this case the artifact removal via notch filtering is more penalizing in assessing muscle performance.

It is finally worth noting that, the ideal case of α motor neuron activated monosynaptically by muscle spindle Ia fiber was assumed. Polysynaptic pathways are however also possible in motor neuron activation, resulting in more variability of the MUAP synchronization within the vibration stimulus and in an increased latency jitter. Hence, in real applications the expected amount of continuous spectrum related to a synchronized MU may be higher than that predicted by this study.

V. CONCLUSION

The derived mathematical formulation well describes the changes observable in the power spectrum of a motor unit action potential train stimulated by vibration accounting for the level of synchronization. It should be underlined that this study deals only with the spectrum of synchronized motor units and not of the whole EMG. Indeed, in a vibrating muscle both synchronized and not synchronized motor units can coexist. The entire EMG spectrum will obviously result from the overlapping of both groups of motor units. However, some WBV studies evaluate the increase in muscle activity by calculating concise EMG parameters (e.g. RMS value): this can lead to error if the motion artifact is not properly removed. Motion artifact spectrum is purely discrete at the harmonics of vibration and can be cancelled by opportune comb notch filters. The results of this study confirm that, by deleting these harmonics, only a relatively small percentage of the synchronized MU spectrum is lost; most of the spectrum is

indeed continuous. In addition, our results strongly recommend to avoid the mere rectification of the raw EMG signal for WBV applications, as it significantly alters the information contained in the spectrum and does not eliminate the artifact. These recommendations can help in more accurate assessment of muscle response to vibratory stimulation

APPENDIX

This appendix reports the complete sequence of mathematical steps to obtain the power spectrum of the MUAPT starting from equation (2) and (3). As previously shown, a single MUAPT $x(t)$ quasi-synchronized with a mechanical vibration stimulus can be written as a specific time sequence of a given MUAP waveform $m(t)$:

$$x(t) = \sum_{k=-\infty}^{\infty} m(t - kT_s - \alpha_k) \quad (8)$$

Hence, the MUAPT signal can be described by:

$$x(t) = r(t) * m(t) \quad (9)$$

Where $r(t)$ is the quasi-synchronized Dirac pulses train (eq. (5)). The autocorrelation of a cyclostationary random process with period T_s (i.e. $r(t)$) can be computed as the time average of the ensemble autocorrelation function:

$$R_r(\tau) = \lim_{L \rightarrow \infty} \frac{1}{LT_s} \int_{-LT_s/2}^{LT_s/2} R_r(t, \tau) dt \quad (10)$$

Where:

$$R_r(t, \tau) = E[r(t) \cdot r(t - \tau)] \quad (11)$$

Therefore

$$R_r(t, \tau) = E \left[\sum_i \sum_j \delta(t - iT_s - \alpha_i) \cdot \delta(t - \tau - jT_s - \alpha_j) \right] \quad (12)$$

By substituting $k = i - j$, the equation becomes:

$$R_r(t, \tau) = \sum_k \sum_i E[\delta(t - iT_s - \alpha_i) \cdot \delta(\tau - kT_s - (\alpha_i(t) - \alpha_{i-k}))] \quad (13)$$

Hence, also $R_r(t, \tau)$ results a periodic function in t with a period T_s , and merging equation (10) and (13) we obtain:

$$R_r(\tau) = \sum_k \lim_{L \rightarrow \infty} \frac{1}{LT_s} \sum_{i=-L/2}^{L/2} \int_{iT_s}^{(i+1)T_s} E[\delta(t - iT_s - \alpha_i) \cdot \delta(\tau - kT_s - (\alpha_i(t) - \alpha_{i-k}))] \quad (14)$$

Consider a new process β , which sequence $\beta_k = \alpha_i - \alpha_{i-k}$. Since α_k is stationary, the statistics of β_k depend only on time difference k . Taking the integration inside the expectation operator and after some manipulations, we obtain:

$$R_r(\tau) = \frac{1}{T_s} \sum_k E[\delta(\tau - kT_s - \beta_k)] \quad (15)$$

Let $P_A(\alpha)$ be the probability density function of the random variable α_k , and let $P_B(\beta)$ be the probability function of the random variable β_k . Hence, by definition of expectation:

$$E[\delta(\tau - kT_s - \beta_k)] = \int_B P_{Bk}(\beta) \cdot [\delta(\tau - kT_s - \beta)] \cdot d\beta = P_{Bk}(\tau - kT_s) \quad (16)$$

By substituting equation (16) in equation (15):

$$R_r(\tau) = \frac{1}{T_s} \sum_k P_{Bk}(\tau - kT_s) \quad (17)$$

Therefore, $P_{Bk}(\tau - kT_s)$ represents a sequence of impulses centered on kT_s . This equation can be rewritten as:

$$R_r(\tau) = \frac{1}{T_s} \sum_k \delta(\tau - kT_s) * P_{Bk}(\tau) \quad (18)$$

The spectrum of the MUAPT $m(t)$ signal can be obtained by Fourier transform of equation (18), $P_{Bk}(b)$ should be evaluated for all k to compute the autocorrelation function $R_r(\tau)$. The values of the sequence α_k are independent and identically distributed random variables, therefore the values α_i and α_{i-k} are independent. The probability density function $P_{Bk}(\beta)$ results to be the convolution of the $P_A(\alpha)$ and $P_A(-\alpha)$ [43].

$$P_{Bk}(b) = \begin{cases} P_A(\alpha) * P_A(-\alpha) = P_B(\beta) & \text{for } k \neq 0 \\ \delta(b) & \text{for } k = 0 \end{cases} \quad (19)$$

By substituting equation (19) in the equation (18) the autocorrelation function becomes:

$$R_r(\tau) = \frac{1}{T_s} (\delta(\tau) - P_B(\tau)) + \frac{1}{T_s} \sum_{k \neq 0} \delta(\tau - kT_s) * P_B(\tau) \quad (20)$$

$S_{rr}(f)$ of the signal $r(t)$ is obtained by taking the Fourier transform of the autocorrelation function $R_r(\tau)$.

Let $A(f)$ be the Fourier transform of $P_A(\tau)$. Since $P_A(\tau)$ is real, the Fourier transform $B(f)$ of $P_B(\tau)$ results:

$$B(f) = A(f) \cdot A^*(f) = |A(f)|^2 \quad (21)$$

$S_{rr}(f)$ then results:

$$S_{rr}(f) = \frac{1}{T_s^2} \sum_k \delta\left(f - \frac{k}{T_s}\right) \cdot |A(f)|^2 + \frac{1}{T_s} \left(1 - |A(f)|^2\right) \quad (22)$$

Finally, $S_{xx}(f)$ of the signal $x(t)$ is given by:

$$S_{xx}(f) = \frac{|M(f)|^2}{T_s} \cdot \left[1 - |A(f)|^2 + \frac{|A(f)|^2}{T_s} \cdot \sum_k \delta\left(f - \frac{k}{T_s}\right)\right] \quad (23)$$

Where $M(f)$ is the Spectrum of the MUAP waveform $m(t)$ (see equation (5)). Equation (23) is equal to the equation (6) in the result section of the main text Q.E.D..

REFERENCES

- [1] M. C. Brown, I. Engberg, and P. B. Matthews, "The relative sensitivity to vibration of muscle receptors of the cat," *J Physiol*, vol. 192, no. 3, pp. 773-800, Oct, 1967.
- [2] J. P. Roll, J. P. Vedel, and E. Ribot, "Alteration of Proprioceptive Messages Induced by Tendon Vibration in Man - a Microneurographic Study," *Experimental Brain Research*, vol. 76, no. 1, pp. 213-222, 1989.
- [3] A. Fratini, A. La Gatta, P. Bifulco, M. Romano, and M. Cesarelli, "Muscle motion and EMG activity in vibration treatment," *Med Eng Phys*, vol. 31, no. 9, pp. 1166-72, Nov, 2009.
- [4] J. M. Wakeling, B. M. Nigg, and A. I. Rozitis, "Muscle activity damps the soft tissue resonance that occurs in response to pulsed and continuous vibrations," *Journal of Applied Physiology*, vol. 93, no. 3, pp. 1093-1103, Sep, 2002.
- [5] M. Cesarelli, A. Fratini, P. Bifulco, A. La Gatta, M. Romano, and G. Pasquariello, "Analysis and modelling of muscles motion during whole body vibration," *Eurasip Journal on Advances in Signal Processing*, vol. 2010, 2010.
- [6] D. Burke, K. E. Hagbarth, L. Lofstedt, and B. G. Wallin, "The responses of human muscle spindle endings to vibration of non-contracting muscles," *J Physiol*, vol. 261, no. 3, pp. 673-93, Oct, 1976.
- [7] J. E. Hall, *Guyton and Hall textbook of medical physiology*: Elsevier Health Sciences, 2015.
- [8] J. E. Desmedt, and E. Godaux, "Vibration-induced discharge patterns of single motor units in the masseter muscle in man," *J Physiol*, vol. 253, no. 2, pp. 429-42, Dec, 1975.
- [9] D. Burke, and H. H. Schiller, "Discharge pattern of single motor units in the tonic vibration reflex of human triceps surae," *Journal of neurology, neurosurgery, and psychiatry*, vol. 39, no. 8, pp. 729-41, 1976.
- [10] S. Homma, "Frequency characteristics of the impulse decoding ratio between the spinal afferents and efferents in the stretch reflex," *Progress in brain research*, vol. 44, pp. 15-30, 1976.
- [11] R. Person, and G. Kozhina, "Study of discharge pattern of human soleus motor units in the tonic vibration reflex," *Neurofiziol Kiev*, vol. 21, pp. 765-772, 1989.
- [12] J. Desmedt, and E. Godeaux, "The tonic vibration reflex and the vibration paradox in limb and jaw muscle in man," Basel: Karger, 1980, pp. 215-242.
- [13] R. Person, and G. Kozhina, "Tonic Vibration Reflex of Human Limb Muscles - Discharge Pattern of Motor Units," *Journal of Electromyography and Kinesiology*, vol. 2, no. 1, pp. 1-9, 1992.
- [14] K. E. Hagbarth, G. Hellsing, and L. Lofstedt, "TVR and vibration-induced timing of motor impulses in the human jaw elevator muscles," *J NeurolNeurosurg Psychiatry*, vol. 39, no. 8, pp. 719-28, Aug, 1976.
- [15] D. J. Cochrane, "The potential neural mechanisms of acute indirect vibration," *Journal of Sports Science and Medicine*, vol. 10, no. 1, pp. 19-30, Mar, 2011.
- [16] A. Fratini, T. Bonci, and A. M. Bull, "Whole Body Vibration Treatments in Postmenopausal Women Can Improve Bone Mineral Density: Results of a Stimulus Focussed Meta-Analysis," *PLoS One*, vol. 11, no. 12, pp. e0166774, 2016.
- [17] F. Di Iorio, M. Cesarelli, P. Bifulco, A. Fratini, E. Roveda, and M. Ruffo, "The effect of whole body vibration on oxygen uptake and electromyographic signal of the rectus femoris muscle during static and dynamic squat," *Journal of Exercise Physiology Online*, vol. 15, no. 5, pp. 18-31, 2012.
- [18] M. Cardinale, and J. Lim, "Electromyography activity of vastus lateralis muscle during whole-body vibrations of different frequencies," *Journal of Strength and Conditioning Research*, vol. 17, no. 3, pp. 621-624, Aug, 2003.
- [19] R. D. Pollock, R. C. Woledge, F. C. Martin, and D. J. Newham, "Effects of whole body vibration on motor unit recruitment and threshold," *Journal of Applied Physiology*, vol. 112, no. 3, pp. 388-395, Feb, 2012.
- [20] L. N. Zaidell, K. N. Mileva, D. P. Summers, and J. L. Bowtell, "Experimental evidence of the tonic vibration reflex during whole-body vibration of the loaded and unloaded leg," *PLoS One*, vol. 8, no. 12, pp. e85247, 2013.
- [21] A. Fratini, M. Cesarelli, P. Bifulco, and M. Romano, "Relevance of motion artifact in electromyography recordings during vibration treatment," *J ElectromyogrKinesiol*, vol. 19, no. 4, pp. 710-8, Aug, 2009.
- [22] A. F. Abercromby, W. E. Amonette, C. S. Layne, B. K. McFarlin, M. R. Hinman, and W. H. Paloski, "Variation in neuromuscular responses during acute whole-body vibration exercise," *Med Sci Sports Exerc*, vol. 39, no. 9, pp. 1642-50, Sep, 2007.
- [23] M. A. Lebedev, and A. V. Polyakov, "Analysis of Surface Emg of Human Soleus Muscle Subjected to Vibration," *Journal of Electromyography and Kinesiology*, vol. 2, no. 1, pp. 26-35, 1992.
- [24] R. Ritzmann, A. Kramer, M. Gruber, A. Gollhofer, and W. Taube, "EMG activity during whole body vibration: motion artifacts or stretch reflexes?," *Eur J ApplPhysiol*, vol. 110, no. 1, pp. 143-51, Sep, 2010.
- [25] O. Sebek, I. Karacan, M. Cidem, and K. S. Turker, "Rectification of SEMG as a tool to demonstrate synchronous motor unit activity during vibration," *Journal of Electromyography and Kinesiology*, vol. 23, no. 2, pp. 275-284, Apr, 2013.
- [26] P. Bifulco, M. Cesarelli, M. Romano, and A. Fratini, "Comments on the article "Rectification of SEMG as a tool to demonstrate synchronous

- motor unit activity during vibration", *Journal of Electromyography and Kinesiology*, vol. 23, no. 5, pp. 1250-1251, Oct, 2013.
- [27] C. J. De Luca, R. S. LeFever, M. P. McCue, and A. P. Xenakis, "Behaviour of human motor units in different muscles during linearly varying contractions," *J Physiol*, vol. 329, pp. 113-28, Aug, 1982.
- [28] K. Lienhard, A. Cabasson, O. Meste, and S. S. Colson, "sEMG during Whole-Body Vibration Contains Motion Artifacts and Reflex Activity," *J Sports Sci Med*, vol. 14, no. 1, pp. 54-61, Mar, 2015.
- [29] F. Negro, K. Keenan, and D. Farina, "Power spectrum of the rectified EMG: when and why is rectification beneficial for identifying neural connectivity?," *Journal of Neural Engineering*, vol. 12, no. 3, Jun, 2015.
- [30] O. P. Neto, and E. A. Christou, "Rectification of the EMG Signal Impairs the Identification of Oscillatory Input to the Muscle," *Journal of Neurophysiology*, vol. 103, no. 2, pp. 1093-1103, Feb, 2010.
- [31] A. Fratini, P. Bifulco, M. Romano, F. Clemente, and M. Cesarelli, "Simulation of surface EMG for the analysis of muscle activity during whole body vibratory stimulation," *Computer Methods and Programs in Biomedicine*, vol. 113, no. 1, pp. 314-322, Jan, 2014.
- [32] H. S. Milner-Brown and R. B. Stein. "The relation between the surface electromyogram and muscular force". *Journal of Physiology*. vol. 246, no. 3, pp. 549-569, Apr 1975.
- [33] C. J. De Luca, A. Adam, R. Wotiz, L. D. Gilmore, S. H. Nawab. "Decomposition of Surface EMG Signals". *Journal of Neurophysiology*. vol. 96, no. 3, pp. 1646-1657, 2006 . doi: 10.1152/jn.00009.2006
- [34] D. Farina, D. Falla. "Effect of muscle-fiber velocity recovery function on motor unit action potential properties in voluntary contractions". *Muscle Nerve*. vol. 37, no. 5, pp. 650-658, May 2008. doi: 10.1002/mus.20948
- [35] Z.A. Riley, M.E. Terry, A. Mendez-Villanueva, J.C. Litsey, R.M. Enoka. "Motor unit recruitment and bursts of activity in the surface electromyogram during a sustained contraction". *Muscle Nerve*. vol. 37, no. 6, pp. 745-53, Jun 2008. doi: 10.1002/mus.20978.
- [36] L. McManus, X. Hu, W.Z. Rymer, M.M. Lowery, N.L. Suresh. "Changes in motor unit behavior following isometric fatigue of the first dorsal interosseous muscle". *Journal of Neurophysiology*. Vol. 113, no. 9, pp. 3186-3196, 2015. doi:10.1152/jn.00146.2015
- [37] M. Gazzoni, A. Botter, T. Vieira. "Surface EMG and muscle fatigue: multi-channel approaches to the study of myoelectric manifestations of muscle fatigue". *Physiological Measurement* vol. 38, R27, 2017. doi: 10.1088/1361-6579/aa60b9
- [38] T. Kapelner, N. Jiang, A. Holobar, I. Vujaklija, A.D. Roche, et al. "Motor Unit Characteristics after Targeted Muscle Reinnervation". *Plos One* vol. 11, no. 2, e0149772, 2016. doi: 10.1371/journal.pone.0149772
- [39] P. Romaguere, J. P. Vedel, J. P. Azulay, and S. Pagni, "Differential activation of motor units in the wrist extensor muscles during the tonic vibration reflex in man," *J Physiol*, vol. 444, pp. 645-67, Dec, 1991.
- [40] P. Lago, and N. B. Jones, "Effect of Motor-Unit Firing Time Statistics on Emg Spectra," *Medical & Biological Engineering & Computing*, vol. 15, no. 6, pp. 648-655, 1977.
- [41] C. J. De Luca, "Physiology and Mathematics of Myoelectric Signals," *Ieee Transactions on Biomedical Engineering*, vol. 26, no. 6, pp. 313-325, 1979.
- [42] Z. S. Pan, Y. Zhang, and P. A. Parker, "Motor Unit Power Spectrum and Firing Rate," *Medical & Biological Engineering & Computing*, vol. 27, no. 1, pp. 14-18, Jan, 1989.
- [43] A. Mood, "Introduction to the Theory of Statistics," McGraw-Hill, New York, NY, 1974.